THE PENNSYLVANIA STATE UNIVERSITY
SCHREYER HONORS COLLEGE

DEPARTMENT OF BIOLOGY

Investigation of Striatal Astrocytes to GABAergic Neuron Conversion In Vivo in Huntington's Disease Mouse Model

KEVIN XU
SPRING 2021

A thesis
submitted in partial fulfillment
of the requirements
for a baccalaureate degree
in Finance
with honors in Biology

Reviewed and approved* by the following:

Aimin Liu
Professor of Biology
Thesis Supervisor

Bernhard Luscher
Professor of Biology
Professor of Biochemistry and Molecular Biology
Honors Adviser

* Electronic approvals are on file.

ABSTRACT

Huntington's disease is an inherited autosomal dominant neurodegenerative disease due to a CAG trinucleotide repeat expansion in the huntingtin gene which leads to excessive polyglutamine sequence stretch, resulting in behavioral and motor deficits from the decrease in striatal GABAergic neurons. The human brain is incapable of sufficient self-repair in either removing the toxic gain of function or regenerating GABAergic neurons. Thus, a possible therapeutic solution to address this deficit would be to replace the neuronal death and dysfunction with new neurons. In this lab, I have analyzed the in vivo conversion technology for AAV-mediated ectopic expression of Neuronal Differentiation 1 (ND1) and Distal-Less Homeobox 2 (Dlx2) transcription factors to convert striatal astrocytes to GABAergic neurons in the R6/2 HD mouse model. Under the transgenic mice model, the R6/2 mouse line's expression of a 1.9-kb fragment from the 5' UTR sequence and exon 1 could accurately reproduce the severe anatomical and behavioral symptoms present in Huntington's disease such as motor abnormalities along with the reduction in neuron concentration in the striatum. Through intracranial and retroorbital injections with the ND1 and Dlx2 treatment, there was evidence of striatal astrocyte conversion into GABAergic neurons. Furthermore, behavioral tests indicated that motor function, spatial learning, and weight loss improved for R6/2 mice treated with ND1 and Dlx2. Given these preliminary results, the astrocyte-to-neuron conversion technology with ND1+Dlx2 transcription factors could potentially be a gene therapy to treat Huntington's disease along with other neurodegenerative diseases; however, further experiments and studies of the treatment outcomes and mechanism need to be conducted in order to better understand its potential and limitations.

TABLE OF CONTENTS

LIST OF FIGURES

ACKNOWLEDGEMENTS

I would like to start by thanking Dr. Gong Chen for his support in providing me the opportunity to work in his lab over the past three years. These valuable experiences as an undergraduate working with cutting edge in-vivo conversion technology for brain repair have enabled me to grow as a researcher in gaining a better understanding of various research techniques and protocols. I initially had the chance to work in the Traumatic Brain Injury project under the direct supervision of my mentor, Zhuofan Lei. I would specifically like to thank Zhuofan for having a tremendous impact on my growth as a researcher in honing my laboratory skills and guiding me through a variety of laboratory procedures. He provided excellent support in helping me better comprehend the mechanisms surrounding astrocyte to neuron conversion via ND1 in a closed head injury model.

Afterwards, I was also especially thankful for the opportunity to transition from the Traumatic Brain Injury project to the Huntington's Disease project since the summer of 2019 while working under the doctoral student, Xiaoyi Hou. Xiaoyi has been an incredible mentor in greatly improving my research and procedural techniques especially when I was working full-time in the summer. She provided guidance in understanding retro-orbital injections for global targeting of astrocytes in various brain regions. She also helped to provide valuable support in the development and planning of my honors thesis up to the end of Chen lab.

Finally, I would also like to recognize the other lab members who have been critical during my work in lab. Many thanks to both Dr. Luscher and Dr. Aimin Liu for being willing to supervise the successful completion of my honors thesis on such short notice with the departure of Dr. Gong Chen prior to my senior year. Given the unfortunate timing with the Covid-19

pandemic and Chen lab closing, I would like to thank Dr. Hedong Li for giving me one month access to the lab so that I had the opportunity to collect additional data prior to my thesis writeup. Furthermore, I sincerely appreciated Dr. Zifei Pei, Ms. Donna Sosnoski, and Ms. Yuting Bai for handling the logistical aspects of Chen lab such as mice care, protocol approvals, and virus productions for the procedures. Lastly, I would like to thank members of the Alzheimer's Disease and Huntington's Disease group, consisting of Zheng Wu, Hui Wang, Abhi Sambangi, Shreya Swaminathan, and Xiaoyi Hou, for all their support over the past three years. I am responsible for all work in my honors thesis, so I was involved in all steps in the data collection process like behavioral testing, perfusion, sectioning, staining, and imaging; however, surgery was performed by Zheng Wu, Xiaoyi Hou, and Zhuofan Lei.

Chapter 1

Introduction

Huntington's Disease

Within the central nervous system, the brain coordinates bodily functions, playing a pivotal role in posture, balance, movement, action, feeling, and memories. Any mutations within DNA sequences or protein structures within neurons can lead to serious cognitive, motor, and behavioral changes. Specifically, Huntington's disease (HD) is an autosomal dominant illness that causes a progressive degeneration of striatal neurons in the brain, leading to a broad spectrum of psychiatric, cognitive, and motor disorders. Those with this disease can experience many symptoms including dementia, personality changes, progressive weight loss, uncontrolled choreatic movements, and unsteady gait. These symptoms stem from over 39 CAG trinucleotide repeat sequence in the coding region of the *IT15* gene, which codes for the huntingtin protein[1-3]. The Huntingtin gene (*HTT*) expansion generates long polyglutamine sequence in the NH_2 terminus of the mutant huntingtin protein which exhibits aggregation of mutant HTT (mHTT)[4,5]. This protein aggregation is induced by the mHTT protein which is more susceptible to cleavages in forming shorter protein fragments that misfold to form inclusion bodies that impede neuronal function. GABAergic medium spiny neurons, a type of inhibitory neuron, are especially vulnerable to HTT accumulation, leading to GABAergic neuron degeneration in the striatum of the basal ganglia (Figure 1). Neuron loss can then further spread across the basal ganglia, a region that plays a key role in movement and behavioral control, and overall cerebral cortex[6].

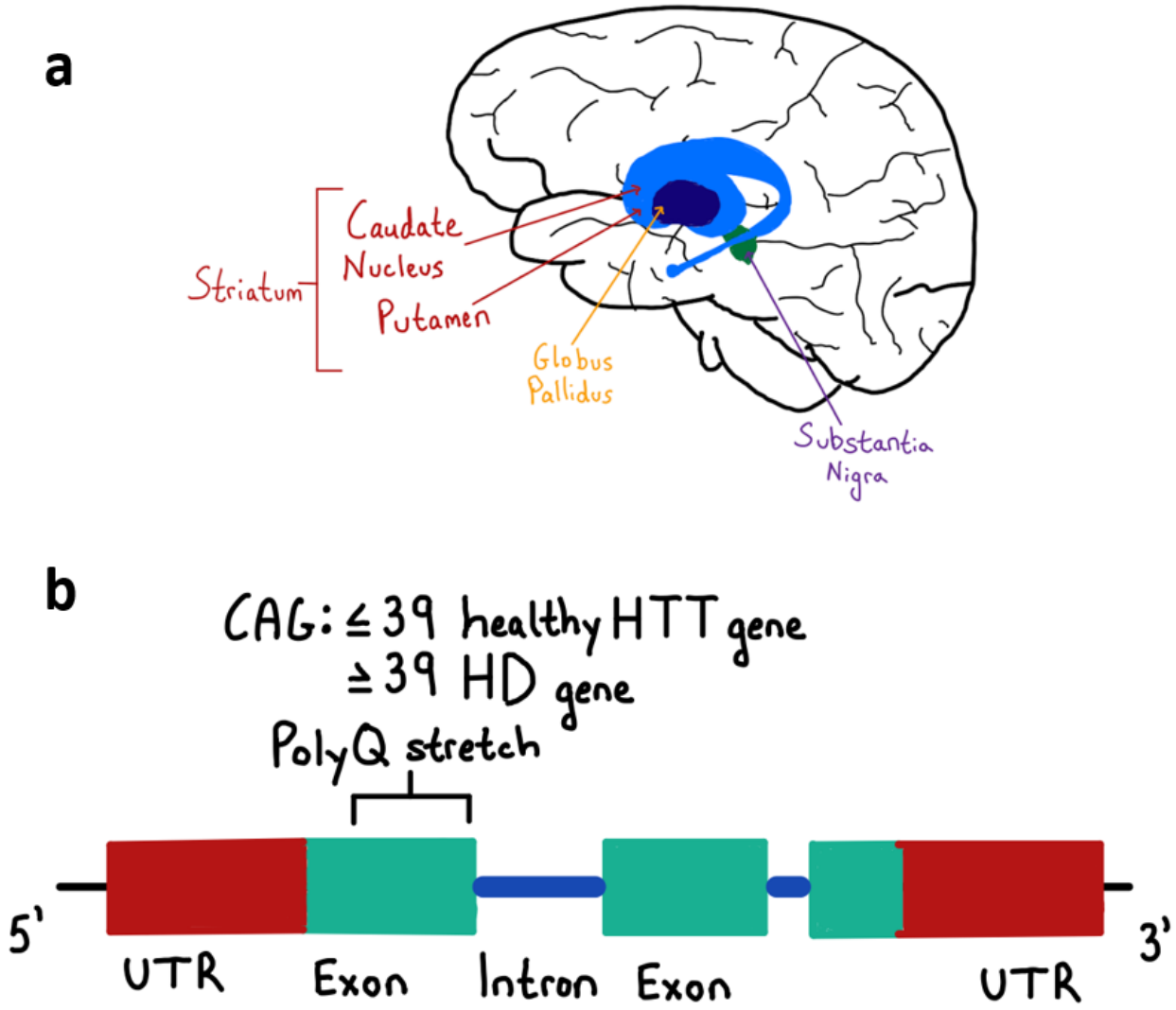

Figure 1: Basic Brain Structure and HTT Protein Affected by Huntington's Disease (**a**) The regional areas of the brain damaged initially by mHTT accumulation include the dorsal striatum which consists of the putamen and caudate nucleus. Neurodegeneration can then spread to other areas such as the basal ganglia which includes the substantia nigra as well as the globus pallidus where striatal medium spiny neurons are especially vulnerable. (**b**) A healthy *HTT* gene contains less than 39 CAG trinucleotide repeats, resulting in less than 39 repeat glutamines in the polyQ region for the cytoplasmic huntingtin protein. However, mutant *HTT* contain more than 39 CAG trinucleotide repeats which leads to expression of a longer polyglutamine tract in the NH_2 terminus of the mutant huntingtin protein.

Patients with Huntington's disease indicate progressive cognitive, psychiatric, and motor symptoms associated with striatum atrophy. These symptoms typically become evident between the ages of 30 to 50 years[7-9]. Less than 10% of patients develop more severe and rapid symptoms of juvenile HD before 20 years of age which usually stem from paternal transmission[10,11]. The earliest symptoms are associated with gradual psychiatric, emotional, and cognitive challenges. These earlier symptoms often lead to changes in sexual behavior, gradual weight loss, and alterations in the circadian rhythm which may be rooted in changes to the hypothalamus[12,13]. As the disease progresses towards the later stages, motor dysfunction and progressive dementia begin to appear with gradual impairment in executive functions such as impaired judgement, comprehension, abstract thinking, and memory[12,14]. The gradual increase in severity of these later stage symptoms can reach a point where HD patients would directly require long term institutional care due to the inability to walk and talk. With the progressive life-threatening dysfunction in motor skills, over 33% of HD patients end up having trouble swallowing which can lead to aspiration pneumonia[15]. Heart disease, the second greatest risk, leads to nearly 25% of deaths for HD patients. Thus, death often takes place within 15 to 20 years after diagnosis of the disease[16-18].

Within the developed world, Huntington's disease is the most pervasive monogenic neurodegenerative disease[19,20]. Overall, there is an estimated five to ten cases of HD per 100,000 people worldwide with the prevalence being close for both men and women. HD is most prevalent in those with a Western European background since it typically affects ten to fifteen individuals within every 100,000 people[21-23]. These new cases are usually inherited from a parent carrying a mutated *HTT* gene, yet nearly 10% of cases stem from new mutations[24]. The disease appears less frequently in those of African or Asian descent given its prevalence of 0.4 for every

100,000 cases[25]. However, higher incidence of HD can occur in certain isolated populations due to local founder effect[26].

Currently, there are no treatments available that can effectively slow the onset or effects of Huntington's disease. Thus, clinical care for patients stems from a multifaceted approach to managing and assessing the symptoms to maximize the patient's quality of life[27]. These therapeutic strategies currently are designed to only lessen the primary symptoms evident in HD such as motor sedatives and psychiatric compounds to manage behavioral deficits; however, these treatments are limited in that they do not directly inhibit or slow the disease progression[28]. Thus, research is currently being conducted to combat the disease through novel means such as gene silencing to lower mutant *HTT* production in various animal models[29]. Tetrabenazine was a drug approved in 2000 to treat the effects of chorea and other movement disorders in HD patients despite the significant side effects. Tetrabenazine inhibits the synaptic vesicular monoamine transporter 2 which decreases monoamine uptake into synaptic vesicles, countering some of the effects of chorea[30-32]. In 2017, deutetrabenazine, a heavier form of tetrabenazine, was approved by the FDA as the first small molecule drug to also treat chorea in HD patients[33]. With the limited number of drugs approved to merely address the symptoms of HD, more effective treatments are needed to directly tackle the root of the inexorable disease progression itself.

Astrocyte-to-Neuron Conversion Mechanism

The discovery of the existence of induced pluripotent stem cells that can differentiate and redevelop into specific cell types in 1961 has opened the doors in the field of neuroscience for potential stem cell therapy especially with limitations of the central nervous system in generating

new neurons[34]. Adding a set of four transcription factors into the nucleus of fibroblasts allowed for reversion back into pluripotent stem cells which can then redevelop into nearly any type of cell in the body[35,36]. With the limited capability for the central nervous system to regenerate neurons in the case of neurodegenerative diseases, the ability for pluripotent stem cells to redevelop into neurons is a technique potentially worth considering. For instance, gamma-Aminobutyric acid producing neurons have been transplanted into various mouse models as possible therapeutic solutions for cases such as Alzheimer's Disease. However, there are several constraints for induced pluripotent stem cells[37-39]. With transplantation of pluripotent cells, there is a possibility that there is immune incompatibility with the host and transplanted cells, which then leads to transplanted cell rejection. Inflammation can also occur through vector toxicity of retrovirus induced pluripotent stem cells, which may be further exacerbated by possible insertional mutagenesis, leading to tumor formation[40,41]. To avoid these potential drawbacks, engineered adeno-associated viral vectors that lack immunogenicity and pathogenicity can be used in vivo to infect certain cell types for the ectopic expression of specific neural transcription factors that align with those of another cell type. This process can allow for the direct conversion of a specific mature cell type to another cell type[42-44].

Since neurodegeneration is a pathological hallmark for injury in the central nervous system, restoring neurons after brain injury is pivotal for brain repair. Through the research conducted in our lab, direct cellular reprogramming in converting local glial cells to neurons in vivo can occur through the expression of specific neural transcription factors in certain differentiated cell types to conform to those of other cell types, which can be performed through the use of a viral vector that directly transfers a certain gene sequence from one cell to another[45-47]. With an ability to proliferate for regenerative purposes, glial cells constitute over 50% of the

overall brain cells[48]. Our lab had successfully demonstrated direct conversion of mature astrocytes into functional neurons in vivo in the mouse brain. Since they make up around 30% of the cells in the central nervous system and surround every neuron, astrocytes can be an effective internal reservoir for cellular reprogramming[49,50]. Specifically, the coexpression of both ND1 and Dlx2 neural transcription factors can directly convert the striatal astrocytes into medium spiny neurons in R6/2 mouse model, a transgenic mouse model that expresses a section of the human *HD* gene under human promoter elements[51]. Neuronal differentiation 1 (ND1) is a member of a basic helix-loop-helix transcription factor family and is present in neurons for neuronal differentiation and generation[52]. Dlx2, containing a homeobox, acts as a transcriptional activator in interneuron differentiation and is pivotal for generating GABAergic neurons[53]. The combination of both ND1 and Dlx2 transcription factors can then drive the conversion of striatal astrocytes into GABAergic neurons in HD mouse models[51].

Given the preliminary in vivo cellular conversion results thus far, this technology opens the door for future possibilities in systematically addressing various neurodegenerative diseases. Since supporting glial cells surround every neuron in mammalian brains, direct glia-to-neuron reprogramming can avoid potential concerns with immunorejection while offering higher neuroregeneration efficiency. Generating new sources of neurons in vivo directly from an individual's glial cells to compensate for cell death or damage can overcome the limited regenerative capabilities intrinsic to the mammalian central nervous system. Thus, our lab has been incorporating such ND1-based gene therapy into various brain disorders such as ALS, stroke, Alzheimer's disease, and spinal cord injury.

Through AAV-based gene therapy, I hypothesize that the use of ND1 plus Dlx2 transcription factors can convert striatal astrocytes to GABAergic neurons which can serve as an

alternative disease-modifying therapy to delay the onset or slow the progression of Huntington's disease. The first section of this thesis details the ability for the combination of ND1 and Dlx2 via intracranial injection to convert astrocytes into neurons in the striatum which was demonstrated at various time points in comparison to the R6/2 mCherry-transduced control group. Another approach to labeling astrocytes with the virus system involving retro-orbital injection was investigated to observe the global infection pattern as well as astrocyte to neuron conversion in the brain and spinal cord of R6/2 mice. The second portion of this thesis examined the phenotypic abnormalities through the use of various behavioral tests to confirm the behavioral deficits in R6/2 mice while also demonstrating statistically significant improvements in motor function, spatial learning, and weight loss reduction for R6/2 ND1+Dlx2 transduced mice.

For the work done in my honors thesis, Ms. Yuting Bai and Dr. Zheng Wu were involved in the breeding and genotyping of the R6/2 mice. Ms. Donna Sosnoski was responsible for protocol approvals, and Dr. Zifei Pei was responsible for AAV5 generation and productions for the experiments. Stereotaxic intracranial surgeries and retro-orbital injections were performed by Dr. Zheng Wu, Mrs. Xiaoyi Hou, and Mr. Zhuofan Lei. I am responsible for all work involving transcardial perfusions, coronal and sagittal tissue sectioning, immunostaining, imaging using the Olympus confocal microscope, behavioral tests, and statistical analysis.

Chapter 2

Materials and Methods

Huntington's Disease Mouse Model

Serving as the Huntington's disease mouse model, the R6/2 transgenic mouse line (B6CBA-Tg(HDexon1)62Gpb/3J, JAX Stock #006494) was developed through B6CBAF1/J males mating with ovarian transplant hemizygous females which were both purchased from Jackson Laboratory. Some four- to six-week-old R6/2 transgenic mice were also purchased from Jackson Laboratory directly. These mice were weaned and then genotyped via PCR using skin samples at three to four weeks of age to determine the existence of the mutation. Both two- to five-month-old male and female littermates with the mutated gene present were used for AAV5 injection. These hemizygous mice were kept in 12:12 hour light and dark cycles with continuous access to water and chow ad libitum. The R6/2 mouse line modeled the pathology of Huntington's Disease in humans through the expression of a 1.9-kb fragment from the 5' UTR sequence and exon 1 with over 120 CAG trinucleotide repeats of human *HTT* gene, resulting in the polyglutamine expansion in huntingtin protein. These neuroanatomical abnormalities worked as an effective mammalian Huntington's disease model where the onset of severe anatomical and behavioral symptoms typically occurred after five to six weeks with the presence of resting tremors, progressive weight loss, and potential cardiac dysfunction and seizures[23]. All experimental protocols and animal experiments were approved by Pennsylvania State University Institutional Animal Care and Use Committees (IACUC) in accordance with guidelines of the National Institutes of Health for the Care and Use of Laboratory Animals.

Viral Vector Delivery Reprogramming Astrocytes to Neurons

Chosen for its preferential astrocyte infection, adeno associated virus 5 (AAV5), packaged with the Cre recombinase enzyme, was used in order to deliver ND1 and Dlx2 transcription factors. The Cre flip-excision (FLEx) system was developed to track the neurons converted from astrocytes in the central nervous system through the Human Glial Fibrillary Acidic Protein (GFAP) promoter that is usually expressed in astrocytes. The system also included a Cre recombinase vector that is only expressed in virus infected astrocytes under the GFAP promoter, stimulating ND1 and GFP or Dlx2 expression. The FLEx vectors contained a coding sequence of either ND1, Dlx2, or mCherry-P2A-mCherry that had its sequence inverted in between double loxP sites. The ND1 and Dlx2 (FLEx-ND1-P2A-mCherry and FLEx-Dlx2-P2A-mCherry) combination worked as the experimental treatment while the FLEx-CAG::mCherry-P2A-mCherry worked as the R6/2 mCherry-transduced control group. Separated by P2A self-cleavage sites, these two genes were packaged with the CAG promotor that was active in all cell types. The Cre recombinase enzyme inverted the coding sequence to its correct orientation for expression to occur (Figure 2). ND1, a transcription factor mostly responsible for glutamatergic neuron generation, and Dlx2, a transcription factor crucial for GABAergic neuron generation, were utilized together to determine whether coexpression could effectively convert specifically striatal astrocytes into GABAergic neurons.

Zifei Pei produced the recombinant AAV used in the lab through the introduction of human embryonic kidney 293T cells. Polyethylenimine transfected pAAV5-RC, pAAV expression vector, and the pHelper for three days in which the cells were then isolated by centrifugation.

Figure 2: Schematic Depiction of AAV5 Framework
GFAP promotor carrying Cre recombinase (GFAP::Cre) inverted the coding sequence to its correct orientation to activate FLEx-CAG::mCherry-P2A-mCherry for mCherry expression in targeting astrocytes.

Brain and Spinal Cord Preparation

A 5 µL Hamilton Syringe containing 2 µL of AAV5 with a 34G needle was used for bilateral intracranial injections. These AAV5 injections were conducted on two to three-month-old R6/2 and wild type mice that were first intraperitoneally injected with 16 mg/kg of xylazine and 120 mg/kg of ketamine to anesthetize them. The mice fur on the head were trimmed, and artificial eye ointment was added to the eyes along with supplemental oxygen to protect the mice over the course of the operation. Incision occurred at the midline scalp with a scalpel to expose portions of the skull for a 1 mm hole to then be drilled into the skull itself for intracranial injection at the striatum region of the brain. Some mice also received CTB injections of 0.5 µg per site in the substantia nigra pars reticulata and globus pallidus which were also areas of striatal medium spiny neuron projections. Once the injection needle was slowly lowered into the 1 mm hole, the injection itself had a constant flow rate of 0.2 µL per minute for a total volume of 2 µL over the course of ten minutes. Following the viral injection, the needle remained in place for over ten minutes before being withdrawn to allow the injected virus to diffuse properly. After stereotaxic viral injection, the midline scalp incision was stitched closed through the use of polyglycocidic acid absorbable sutures. The treated mice were then placed in clean cages with heating pads to recover post-surgery.

Beyond multi-site intracranial injection of AAV5 to achieve global cell targeting, another approach to reach global astrocyte targeting for conversion involved the retro-orbital route. Retro-orbital injection in the medial canthus was one type of intravenous delivery route for global astrocyte targeting for conversion. The mice were first placed in a Plexiglas chamber for isoflurane to anesthetize the mice. The anesthetized mice were then placed in a left lateral recumbency position on a nose cone attached to a non-rebreathing apparatus while on top of a heating pad. Gentle pressure was applied to the skin that was ventral and dorsal to the eye for the mouse's right eye to slightly protrude. Ophthalmic anesthetics were also applied to the right eye before a 27.5G needle was inserted bevel down at 30^{o} into the medial canthus to reach the retro-orbital sinus which was a pool of several vessels. The injection was completed for the needle to then be withdrawn smoothly and slowly to give the virus time to disseminate through the circulatory system so that it would not follow the needle path out. Once the procedure was completed, the mouse was placed back into a clean cage with heating pads until the mouse regained consciousness.

For tissue preparation, the mice were administered 2.5% Avertin (1 g of 2-2-2-tribromoethanol and 1 mL of 2-methyl-2-butanol in 39 mL of 1xPhosphate Buffer Solution) through intraperitoneal injection to first deeply anesthetize the mice (0.5 mL for males, 0.4 mL for females). To perform transcardial perfusion, the deeply anesthetized mice were then securely attached to a cork board ventral side up and cut through the sternum area to access the ribcage and diaphragm which were then moved aside to access the heart. The left ventricle of the heart was penetrated with a 28-gauge needle to pump cold artificial cerebrospinal fluid (aCSF) in order to drain away the blood. The right atrium of the heart was also immediately cut to drain blood from the circulatory system to allow aCSF to flow through the body. Once the liver and tongue

turned sufficiently pale after enough blood was drained, the aCSF pump was turned off to then remove the brain. The spinal cord was also removed for retro-orbital injected mice since the retro-orbital route globally targeted astrocytes in the central nervous system for conversion. Following perfusion, the brains were kept in 4% paraformaldehyde at 4ºC in darkness overnight. The spinal cord samples also followed this preparation but then had to be dehydrated in 30% sucrose over the course of three days. The brain samples were then coronally cut via a vibratome into 30 μm slices. For the spinal cord, the samples were frozen in a cryomatrix block that were then sagittally or coronally sectioned into 30 μm slices with a Leica Cyrostat through manually running a blade across a positively charged glass slide. Sliced samples were then kept in -30ºC cold rooms for longer term storage.

Immunofluorescent Staining and Microscope Imaging

Immunostaining is a method used to be able to visualize certain cell markers in a sectioned tissue sample. The brain slices were first washed with phosphate buffer solution (PBS, OSM: 302, pH 7.28) three times for a total of 30 minutes. 150 μL of blocking buffer which contained 5% normal donkey serum (NDS) and 0.3% triton PBS was washed with the samples to inhibit non-specific binding sites for two hours. After removal of blocking buffer, primary antibody solutions were diluted in accordance with their appropriate ratios in 5% NDS and 0.05% triton PBS and then added to the samples to be incubated at 4ºC for 48 hours. After incubation for two nights, the samples were washed three times in PBS for the samples to then be incubated for two hours at room temperature with the appropriate secondary antibody solution conjugated with Alexa 405, 488, 647 and diluted to a 1:500 concentration in 5% NDS and 0.05%

triton PBS. The samples were then washed three times with PBS after secondary antibody incubation to then be mounted in antifading mounting solution on glass slides with coverslips sealed with nail polish. The slides were left to dry for one day in the dark at room temperature before storing them in the cold room. All fluorescent images were taken using the Olympus Confocal Laser Scanning microscope for 20x magnification and 40x magnification using an oil lens.

Behavioral Tests

In preparation for the behavioral test, all mice were individually housed in separate cages and acclimated to the animal room for over an hour to lessen potential stresses present in the mice due to cage movement. For the behavioral tests, there were four experimental groups consisting of wild type, R6/2, mCherry transduced R6/2 mice acting as control, and ND1 plus Dlx2 treated R6/2 mice. Within each group, five mice were used consistently across all behavioral tests performed and included both male and female mice. Specifically, both the wild type and the R6/2 ND1 plus Dlx2 transduced group consisted of three male and two female mice, the R6/2 group consisted of four males and one female, and the R6/2 mCherry-transduced control group consisted of two males and three females. The mice were injected at six weeks so behavioral tests were conducted four weeks post injection when the mice were ten weeks of age which allows sufficient time for the symptoms of Huntington's disease related to neurodegeneration as well as the potential effects of the ND1 plus Dlx2 treatment for in-vivo cell conversion to appear. All behavioral tests were conducted in the dark phase under red light at 8 PM due to evidence indicating that the light phase induced greater cognitive and behavioral

disruptions in mice undergoing behavioral experiments[54]. The open field test was conducted first at the start of when the mice were 10 weeks of age all in the same day. The Y-maze behavioral test was conducted five days after the open field test to provide time for the mice to rest and recover.

The open field test consisted of an open-top white box of 50 x 50 x 30 cm in dimension where the mouse was carefully placed in the center of the box at the start of the five-minute recording. Thus, the mouse freely moved within the enclosure of the box during that time frame to then be analyzed for locomotor levels. Each five-minute trial was recorded to then be analyzed for total distance traveled between the various experimental groups through a computer program called EthoVision XT, Noldus which was calibrated to the open-top white box in order to track, analyze, and record the movement of the mice. Between each animal test, the white box was thoroughly cleaned with 70% ethanol to remove potential scent cues from the previous test.

Y-maze consisted of three radial arms joined at 120-degree angles at the center in the shape of the letter 'Y'. Each arm was 10 cm high, 5 cm wide, and 35 cm long. Each mouse was placed in the center of the Y-shaped apparatus between the arms for it to be able to explore the maze for five minutes. The pattern and number of entries in the three arms were recorded for all experimental groups to determine the memory deficits for each mouse. Thus, repeated entries into the same few arms indicated poorer memory performance while more consistent alternations between all three arms indicated memory of the previous arm visited. Like the open field test, the y-maze apparatus was thoroughly cleaned with 70% ethanol after each five-minute trial to remove any scent cues from the prior mouse.

Mouse weight specifically for the R6/2 mice provided in either the R6/2 mCherry transduced control or ND1 plus Dlx2 treatment was measured at two time points of one week

before surgery and six weeks post-surgery. This measurement was conducted since the R6/2 mouse model has shown to display progressive weight loss of up to a 20% decrease in weight after 12 weeks[23]. Each mouse was weighed individually under an approved vent hood in the animal room on Friday's at 8:00 PM.

The statistical analysis to quantify the results of the various behavioral tests performed along with the graphical depiction of the data either in the form of mean ± standard error of the mean (SEM) or a box and whisker plot was done using a software called GraphPad Prism 9.0. The statistical significance and p-value were analyzed through the use of one-way ANOVA test followed by a post-hoc Dunnett test for comparisons between the three different types of R6/2 mice with the R6/2 mice as the reference group. Unpaired two-tailed Student's t-tests were also performed to analyze the statistical significance within two-group comparisons between wild type and R6/2 mice.

Chapter 3

Results

Striatal Astrocyte to GABAergic Neuron Conversion via ND1 and Dlx2

Since astrocytes surround nearly every neuron in the brain, they were seen as a potentially viable natural source for cell conversion. Thus, two time points of 11 and 17 weeks were taken to evaluate the basic characterization of the R6/2 mouse model specifically in the striatum which has shown to be especially vulnerable to neuron loss due to mHTT accumulation. Even at 11 weeks, neurodegeneration at the striatum was evident for the R6/2 mice when compared to the wild type mice at that same time point which aligned with features of the R6/2 mouse model that had over 40% reduction in brain and striatal volume by 12 weeks[23]. By 17 weeks, neurodegeneration had advanced to a more severe stage in which greater neuron loss in terms of quantity and concentration occurred in the striatum for the R6/2 mouse (Figure 3a). Higher concentrations of S100β+ astrocytes were also observed surrounding neurons in the striatum for both wild type and R6/2 mice, confirming its presence surrounding neurons as a potential reservoir for conversion. In the ND1 plus Dlx2 transduced R6/2 mice (AAV5 GFAP-Cre+CF/ND1 Dlx2 mCh), stereotaxic intracranial injections occurred at 6 weeks so two time points were taken at 5- and 11-weeks post injection (wpi) in order to be able to compare the markers with the wild type and R6/2 group. After 5 wpi, neuron concentration appeared to have increased in the striatum when compared to the R6/2 11-week time point. By 11 wpi, even higher neuron concentration was observed along with a further reduction in intensity for the GFAP marker for astrocytes, indicating that astrocyte to neuron conversion likely occurred in the process of neuron regeneration in the striatum (Figure 3b).

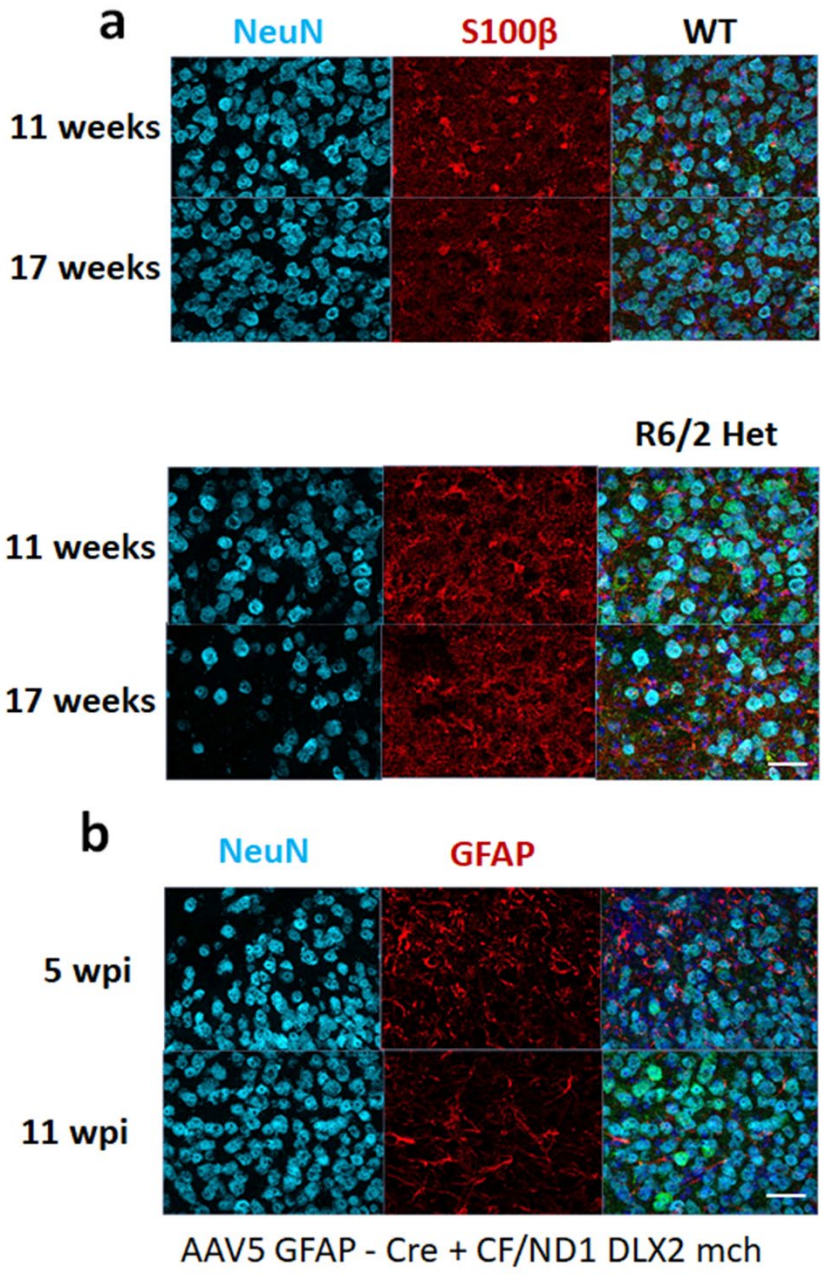

AAV5 GFAP - Cre + CF/ND1 DLX2 mch

Figure 3: Characterization of R6/2 model for Neuron Concentration in Striatum
(**a**) Overview of neuron concentration in the striatum for wild type and R6/2 mice after 11 and 17 weeks. With the decrease in the presence of NueN, a neuronal nucleus marker, at 11 weeks and especially at 17 weeks, severe neurodegeneration occurred in the striatum which matched the characterization of the R6/2 mouse model. High concentration of S100β+ astrocytes were observed surrounding NeuN in both groups, confirming its potential as a natural reservoir. Scale bar is 20 μm. (**b**) R6/2 mice treated with ND1+Dlx2 (AAV5 GFAP-Cre+CF/ND1 Dlx2 mCh) at 6 weeks showed greater concentrations of NeuN when compared to the R6/2 mice at the same time points. NeuN concentration increased further at 11 wpi along with a decrease in GFAP astrocyte intensity, indicating a shift from a more astrocytic population to a mixed population of neurons and astrocytes. Scale bar is 20 μm.

To further test the effects of ND1 plus Dlx2 in the R6/2 mouse model, AAV5 C-F-mCh-P2A-mCh+GFAP-Cre1/3 for the control group and AAV5 C-F-ND1/Dlx2-P2A-mCh+GFAP-Cre1/3 for the experimental group were intracranially injected in the striatum of R6/2 mice. R6/2 mice were injected at eight weeks of age and sacrificed two weeks post injection (wpi) to analyze the infection patterns. Two weeks after the ND1 plus Dlx2 treatment, the GFP+ cells in the ND1 group were morphologically neuron-like with those cells also colocalizing with ND1, GFP, and NueN as denoted by the white arrows. However, in the R6/2 mCherry-transduced control, the GFP+ cells remained astrocytic in nature and did not colocalize with the other markers (Figure 4a). Thus, the AAV5 GFAP::cre system was able to target astrocytes such that apparent astrocyte to neuron conversion could be observed two weeks after the ND1 plus Dlx2 treatment when compared to the R6/2 mCherry-transduced control group.

In a separate experiment, the AAV Cre-FLEx system was tested over various time points to better understand and observe the changes in the conversion from astrocyte to neurons in the striatum. AAV5 GFAP::cre was added with CAG::ND1-P2A-mCherry and AAV5-CAG::Dlx2-P2A-mCherry that was then intracranially injected into the striatum of adult wild type mice at three months old. Four time points of 7-, 14-, 21-, and 35-days post injection (dpi) were analyzed, and it was found that there were little mCherry+ cells showing NeuN+ signal after

ND1 plus Dlx2 coexpression in the earlier time points in the 7 and 14 dpi since at that time point, most of the viral infected mCherry+ cells were GFAP+ astrocytes in the striatum. As the time point increased towards 35 dpi, there appeared to be a trend in which less mCherry+ cells were colocalizing with GFAP+ astrocytes since more mCherry+ cells were colocalizing with NeuN instead as depicted with the white arrows. This trend suggests that ND1 and Dlx2 coexpression can convert striatal astrocytes into GABAergic neurons (Figure 4b).

With the successful conversion of striatal astrocytes into GABAergic neurons in wild type mice, further experiments using this approach were conducted on the R6/2 transgenic mouse model in order to better understand the regeneration of GABAergic neurons in the case of Huntington's disease. This time, AAV5 ND1 plus Dlx2 for the R6/2 treatment group and the AAV5 mCherry as the control group were injected into the striatum of R6/2 mice after 9 weeks such that the neurological phenotypes underlying Huntington's disease would be present at the time of the intracranial surgery. Both the mCherry transduced control and ND1 plus Dlx2 transduced R6/2 mice were sacrificed at 4 weeks post injection (wpi). In the R6/2 mCherry transduced control group, the infected mCherry+ cells appeared morphologically astrocytic in nature as evidenced by the immunopositivity for S100β as marked by the white arrows. On the other hand, the ND1 plus Dlx2 transduced R6/2 mice had mCherry+ infected cells that were more co-labeled with NeuN instead of S100β as marked with the white arrows. This contrast between the R6/2 mCherry-transduced control and R6/2 ND1+Dlx2 transduced mice suggested that striatal astrocytes can be efficiently converted into GABAergic neurons even in the R6/2 mouse model (Figure 4c).

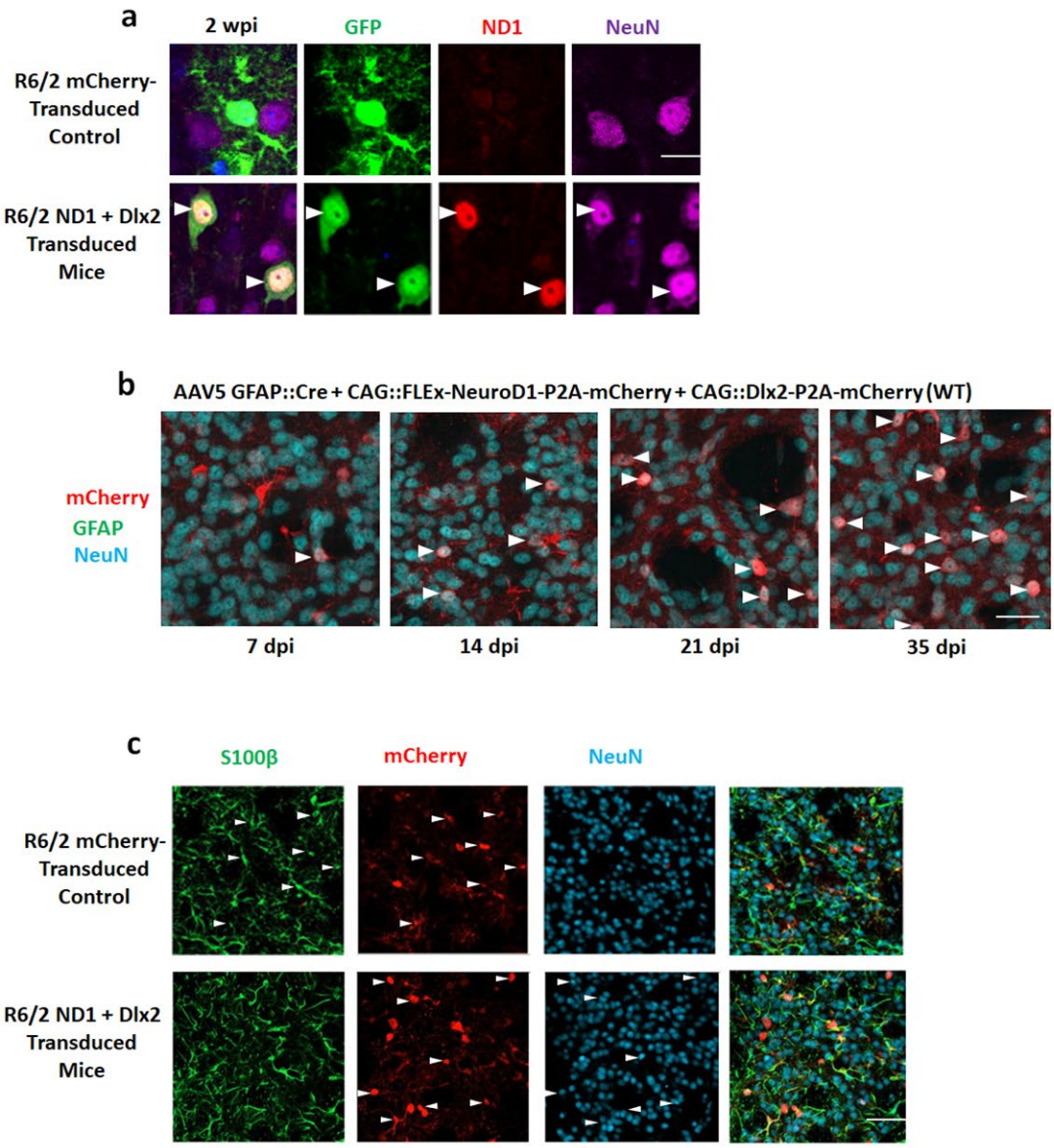

Figure 4: Characterization of In Vivo Striatal Astrocyte to GABAergic Neuron Conversion
(**a**) R6/2 mice were intracranially injected at the striatum as either control (AAV5 C-F-mCh-P2A-mCh+GFAP-Cre1/3) or experimental (AAV5 C-F-ND1/Dlx2-P2A-mCh+GFAP-Cre1/3) group at 6 weeks. At 2 wpi, the GFP+ cells in the R6/2 mCherry-transduced control group remained morphologically astrocytic while the R6/2 ND1+Dlx2 transduced group had GFP+ cells that were morphologically neurons with colocalization of GFP, NeuN, and ND1 based on the 2 white arrows shown. Scale bar is 10 µm. (**b**) 4 images of the 4 different time points over the course of 5 weeks that depict the gradual morphological shift from striatal astrocytes to GABAergic neurons in the striatum

for wild type mice. In the early time points post injection, more of the mCherry+ cells were co-localized with GFAP astrocytes in green while the later time points indicate greater colocalization with NeuN in blue instead of GFAP as marked with the white arrows. Scale bar is 40 μm. (**c**) Depiction of striatum of R6/2 mice injected with either AAV mCherry control or AAV ND1+Dlx2 treatment at 9 weeks and then sacrificed 4 wpi. In the R6/2 mCherry-transduced control group, it appeared that mCherry+ cells co-labeled with S100β in green as marked by the white arrows. However, in the R6/2 ND1+Dlx2 transduced group, mCherry+ cells co-labeled with NeuN in blue instead as marked by the white arrows. Scale bar is 80 μm.

Beyond labeling astrocytes with a virus system through intracranial injection, another approach to reach global astrocyte targeting for conversion involved the retro-orbital route which was viewed as a less invasive method. Retro-orbital (RO) injection belonged to intravenous delivery routes in which the needle was inserted at the medial canthus to reach the retro-orbital sinus for the injectate to circulate in the blood circulation system of the mouse. Thus, retro-orbital injection was used to deliver AAV transcription factor-based therapy to convert astrocytes into neurons. Specifically, AAV PHPeb serotype was chosen because it was reported to have higher efficiency in crossing the blood-brain barrier (AAV PHP.eb GFAP::Cre + AAV PHP.eb CAG::FLEX virus).

In this new set of experiments, a new virus construct was also used with the EF1α promoter directly driving ND1-GFP. The EF1α, Elongation Factor 1α, gene is expressed in both astrocytes and neurons. R6/2 mice underwent retro-orbital injection at 7 weeks of age and were then sacrificed at 3 weeks post injection (wpi). Samples were either treated with AAVeB Ef1α - ND1-GFP or AAVeB GC+CF-ND1+Dlx2 – GFP in order to compare the global infection conditions with some basic markers across the central nervous system from the retro-orbital route. When checking the infection condition in the cervical region of the spinal cord, it was clear that different virus systems targeted different regions. For samples treated with Ef1α-

promoter driven-ND1-GFP, the dorsal region appeared to be more infected in comparison to the ventral portion of the spinal cord. In contrast, for the cre-FLEx system, it appeared to be the reverse in which the ventral portion appeared to be more infected in comparison to the dorsal section of the spinal cord (Figure 5a).

Global infection in the brain was then examined from a sagittal view. In the AAV PHP.eb FLEx-GFP sample 3 wpi, the cre-FLEx system reached a wide range for virus infection in multiple brain regions with some preferential labeling in the cerebral cortex, pons and medulla, and hippocampus regions with less infection in the caudoputamen and striatum which indicated that the retro-orbital route could be an effective means for global astrocyte targeting (Figure 5b).

To examine these regions in more detail, stained cortical markers in the lateral portion of the motor cortex were analyzed in three sets of conditions with wild type, control group in AAVeB GC+CF-ND1-GFP treated R6/2 mice, and treatment group in AAVeB GC+CF-ND1+Dlx2-GFP treated R6/2 mice. When examining NeuN across the seven layers in a column view from the corpus callosum to the top of the cortex, it appeared that the R6/2 mice had thinner layers in the motor cortex compared to those of wild type, indicating potential cortical atrophy from neurodegeneration in the R6/2 mouse brain. Remarkably, the R6/2 ND1 plus Dlx2 transduced group visibly showed higher NeuN density in the layers of the motor cortex which suggests that in-vivo astrocyte-to-neuron conversion therapy can reduce cortical atrophy in R6/2 mice. When examining the GFP marker, it appeared that the R6/2 ND1 plus Dlx2 transduced mice showed the highest infection rate with the highest rate of converted neurons while also showing some astrocytes, suggesting that the RO route can effectively target astrocytes in the cortical region for conversion. For the Cux1 marker, a cortical layer neuron marker specifically for the superficial layer in layers 1 and 2, the control R6/2 mice showed the Cux1 marker in

much weaker intensity which may be due to cortical degeneration from neuron loss when compared to the superficial layers in wild type. However, the Cux1 marker appeared slightly more intense in the R6/2 ND1 plus Dlx2 transduced group, indicating that the in-vivo cell conversion may have restored some neurons in the superficial layer of the motor cortex (Figure 5c).

Lastly, the striatum was also examined to check the infection status for RO injection. In this case, the ChAT marker was used since it is not a cortical layer marker. Instead, it involves choline acetyltransferase, the enzyme that is responsible for biosynthesis of the neurotransmitter acetylcholine. Thus, the majority of acetylcholine is synthesized locally at nerve terminals where ChAT catalyzes the transfer of an acetyl group from acetyl coenzyme A to choline. ChAT is expressed by cholinergic neurons mainly in the striatum and basal ganglia. For the ND1 plus Dlx2 treated R6/2 mice, there were GFP and ChAT double positive cells co-labeled with NeuN as marked by the white arrows, indicating that there were converted cholinergic neurons present in the striatum (Figure 5d). This demonstrates how the ND1 plus Dlx2 treatment via retro-orbital injection could also regenerate cholinergic neurons in the striatum.

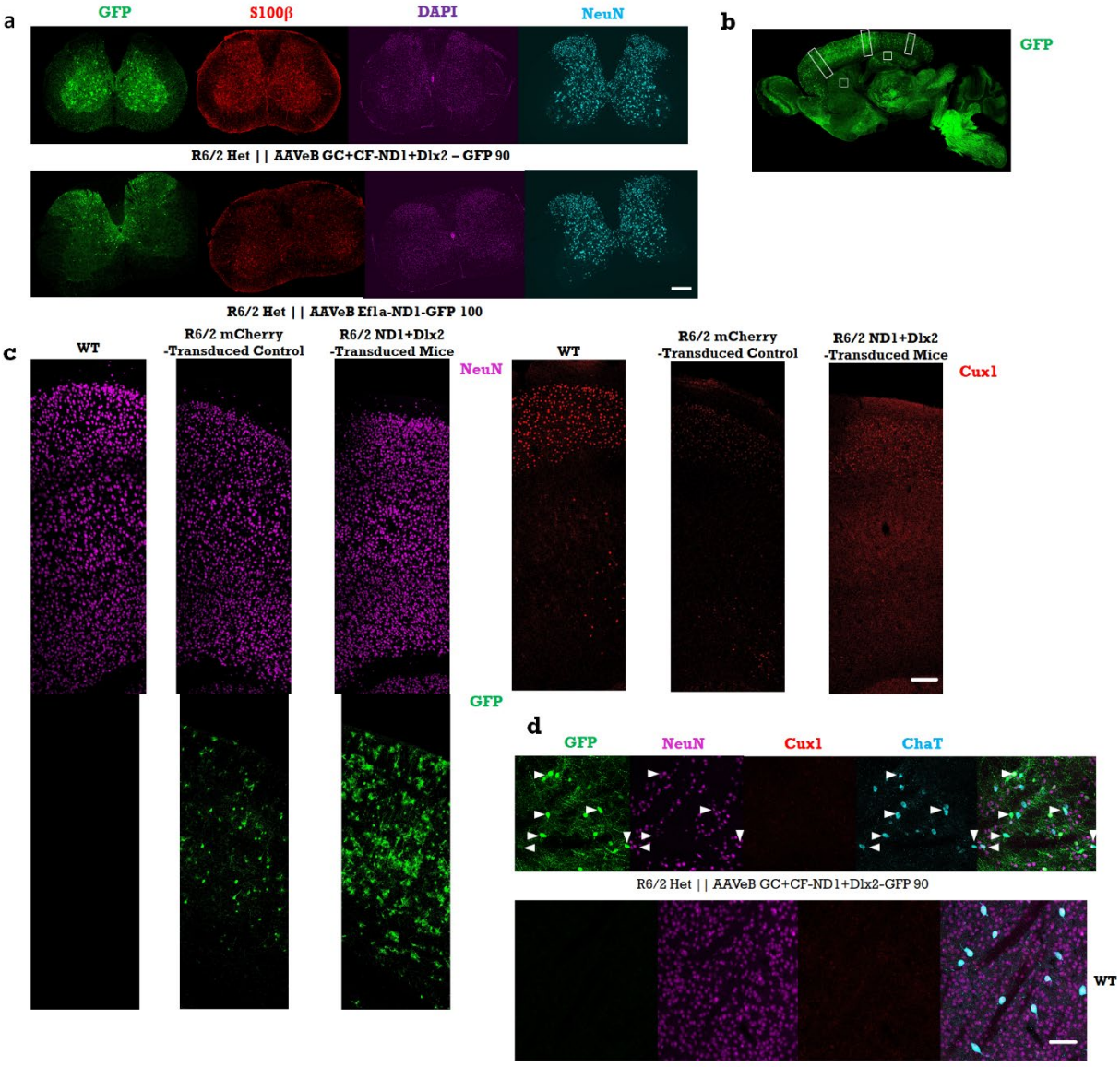

Figure 5: Analyzing Infection Condition in the Spinal Cord and Stained Cortical Markers for Retro-orbital Injection

(**a**) Infection condition in the cervical section of the spinal cord from RO injection in R6/2 mice. For the R6/2 mice treated with Ef1α-promoter driven-ND1-GFP, the dorsal appeared to be more infected in comparison to the ventral portion of the spinal cord while for the cre-FLEx system, it appeared to be the reverse. Thus, different virus systems targeted different regions in global infection. Scale bar is 200 µm. (**b**) Sagittal section of an R6/2 mouse brain treated through RO injection with AAVeB GC+CF-ND1-GFP. White boxes marked indicated areas focused on with higher magnification. Cre-FLEx system reached wide range virus infection in multiple brain regions with preferential labeling in the cortical, hippocampus, pons and medulla regions. (**c**) Higher magnification of stained cortical markers in the motor cortex. Motor cortex in R6/2 mice appeared to be slightly thinner across the 7 layers in comparison to wild type. Slight recovery in NeuN density with the R6/2 ND1+Dlx2 transduced group. R6/2 ND1+Dlx2 transduced group showed the highest infection and converted neuron rate in the GFP marker. The control group had low Cux1 signal due to neurodegeneration in the superficial layer in comparison to wild type which was slightly recovered in the R6/2 ND1+Dlx2 transduced group. Scale bar is 150 µm. (**d**) Stained cortical

markers in the striatum for ND1+Dlx2 treated R6/2 mice showed GFP and ChAT double positive cells that co-labeled with NeuN as marked by the white arrows which indicated the presence of converted cholinergic neurons from the RO injection. Scale bar is 50 μm.

Behavioral Performance Analysis for Neuron Conversion in R6/2 Mouse Model

Given how the transgenic mouse model expressed exon 1 of the human *mHTT* with over 120 CAG trinucleotide repeats, the R6/2 mice demonstrated progressive behavioral and neurological phenotypes that effectively matched many of the macroscopic symptoms seen in patients with Huntington's Disease. Thus, a series of behavioral tests were conducted to be able to better quantify and visualize the phenotypic differences between wild type and R6/2 as well as determine if R6/2 mice treated with ND1 plus Dlx2 transcription factors for in-vivo cell conversion demonstrated any statistically significant improvement in performance over the R6/2 mCherry-transduced control.

The first behavioral test conducted involved the open field test which assessed locomotive ability. A clinical presentation feature of Huntington's disease involved the atrophy of skeletal muscle due to mHTT proteins forming inclusion bodies in myocytes of R6/2 mice[48]. To quantify the severity of the skeletal muscle wasting and effects of the ND1 plus Dlx2 treatment, the open field test quantified the total distance traveled by the different experimental groups over the course of five-minute trials. In comparison with the wild type group which had an average total distance traveled of 1,702 ± 46 cm, R6/2 mice showed a sharp decrease in total travel distance with an average total travel distance of only 449.5 ± 28 cm ($p < 0.001$; unpaired Student's t-test; Figure 6a). There also appeared to be a pattern in which R6/2 mice spent much

more of the trial at the edge of the box in comparison to the wild type and R6/2 ND1 plus Dlx2 transduced group. This indicated higher anxiety levels for R6/2 mice since the outer walls were considered safe while the center quadrant of the box was considered unsafe for mice. There was no statistically significant difference between the R6/2 group and the R6/2 mCherry-transduced control which had a similar average total distance of 465.25 ± 47 cm. The ND1 plus Dlx2 treated R6/2 mice exhibited a notable increase in distance traveled with an average total travel distance of 1067 ± 270 cm especially when compared to the R6/2 group's travel distance of 449.5 ± 28 cm ($p < 0.001$; one-way ANOVA with post-hoc Dunnett test; Figure 6a). By having over double the average total travel distance in comparison to the R6/2 or R6/2 mCherry-transduced control group, the R6/2 ND1 plus Dlx2 treatment for in vivo cell conversion in R6/2 mice showed notable improvements in locomotive function as suggested by the five-minute trial data.

Beyond motor functions, the short-term memory, spatial learning, and spontaneous alternations of mice were also measured through the use of the Y Maze Spontaneous Alternation test. This behavioral test measured the willingness of mice to explore new settings since healthy wild type mice usually prefer to enter a different arm of the maze instead of repeatedly entering the same arm. Thus, the test involved the septum, prefrontal cortex, basal forebrain, and hippocampus in mice. The test was quantified through a methodology involving manually comparing the third entry to the previous two entries. The three arms in the Y maze were each labeled either Lane A, B, or C. If the third entry was different from the previous two entries, then that particular entry was marked as correct. However, if the third entry involved going back to one of the previous two entries, then that particular entry was marked as an error. Entry into a particular arm was determined based upon the requirement that all four limbs of the mouse must be inside the area of that arm in order to be marked as a legitimate entry. The alternation

percentage was calculated through the formula of $1 - \frac{\text{sum of error value}}{\text{total entry count}}$ for each of the five-minute trials. Thus, the higher the alternation percentage then the lower the error rate, indicating better spatial working memory[55]. The wild type group had the highest average alternation percentage of 74 ± 9.6% especially when compared to the R6/2 group which had drastically lower alternation percentage of 32 ± 7% ($p < 0.001$; unpaired Student's t-test; Figure 6b). There was no statistically significant difference between the R6/2 group and the R6/2 mCherry-transduced control which had a similar alternation percentage of 34.3 ± 6.7%. These data indicated that the error rates were much higher in the R6/2 and R6/2 mCherry-transduced control group which suggested that the frequencies of repeated entries into the same arm were much higher, implying that there was greater impairment in spatial working memory for the R6/2 and R6/2 mCherry-transduced control group. It was also noted during the five-minute trials that the R6/2 mice were observed to have stayed in the center of the Y maze apparatus in between all three arms for a much greater period of time proportionally so fewer total entries were observed which may be tied to symptoms of impaired motor function and skeletal muscular atrophy. Interestingly, the ND1 plus Dlx2 treated R6/2 mice showed significant improvement when compared to the R6/2 group with an average alternation percentage value of 53.3 ± 8.8% ($p < 0.01$; one-way ANOVA with post-hoc Dunnett test; Figure 6b). This increase in alternation percentage suggested that the in vivo astrocyte-to-neuron conversion treatment may have improved the short-term memory and spatial learning for the R6/2 mice.

Finally, the body weight for the various treatment groups were also examined since weight loss was one of the most common peripheral symptoms shown in individuals with Huntington's disease[48]. However, the underlying mechanism in terms of how the mHTT protein exactly affected peripheral tissues to cause progressive weight loss has not been conclusively

determined thus far. With the R6/2 mouse model, these transgenic mice were reported to begin progressive weight loss at eight weeks of age. Thus, for this examination, the body weights for R6/2 mice in either the mCherry transduced control group or ND1 plus Dlx2 transduced group were first measured one week prior to surgery when the mice were at five weeks of age and then measured again six weeks post-surgery when the mice were twelve weeks of age. This particular setup was done before the onset of the weight loss symptoms of HD to determine if there were any major differences in terms of body weight between the R6/2 ND1 plus Dlx2 transduced mice and R6/2 mCherry-transduced control group prior to surgery. The second weight measurement was taken six weeks after surgery in order to be able to provide sufficient time for the effects of the different treatments and HD symptoms to appear. Based on the box and whisker plot, there was no statistically significant difference between the R6/2 mice one week prior to surgery since the average weights for the R6/2 mCherry-transduced control and R6/2 ND1 plus Dlx2 transduced mice were 23.8g and 24.0g respectively ($p = 0.392$; Figure 6c). After six weeks post-surgery, the ND1 plus Dlx2 treated R6/2 mice showed less weight loss when compared to the R6/2 mice treated with mCherry control. The R6/2 mCherry-transduced control group had an average body weight of only 17.6g after six weeks while the R6/2 ND1 plus Dlx2 transduced mice had an average body weight of 20.6g (unpaired Student's t-test; $p = 0.029$; Figure 6c). Thus, through the results from the three behavioral tests, the data may indicate that the ND1 plus Dlx2 treatment in R6/2 mice for in vivo conversion of striatal astrocytes to GABAergic neurons showed potential in improving the neurological and behavioral deficits and slowing the onset and severity of the HD symptoms.

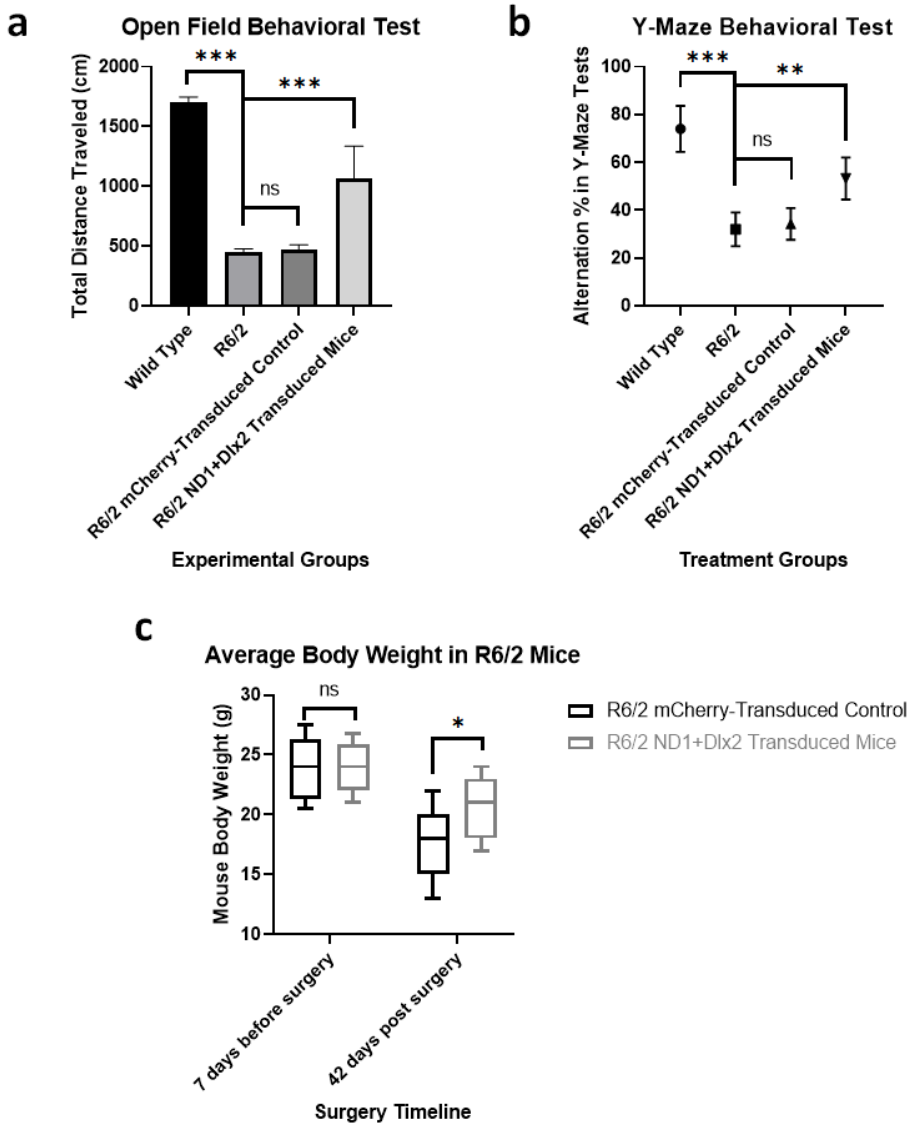

Figure 6: Graphical Comparison Indicating Behavioral Improvements in R6/2 ND1+Dlx2 Transduced Mice (**a**) Graphical depiction of the open field behavioral test data indicated the total average travel distance measured in cm in five-minute trials for each of the four experimental groups. Total average travel distance was much lower for R6/2 in comparison to the wild type (***$p < 0.001$; unpaired Student's t-test for WT and R6/2 comparison). Fortunately, total average distance traveled notably increased for R6/2 mice treated with ND1+Dlx2. The graph provides the data in the format of mean ± SEM (one-way ANOVA with post-hoc Dunnett test for R6/2 mice comparison; ***$p < 0.001$). (**b**) Quantified data of the Y Maze Spontaneous Alternation test measured the alternation percentage based on the formula of 1 - (sum of error value)/(total entry count) in each five-minute trial for all four experimental groups. Alternation percentage was much lower for R6/2 group in comparison to the wild type, indicating a higher error rate (***$p < 0.001$; unpaired Student's t-test for WT and R6/2 comparison). Remarkably, the ND1+Dlx2 treated R6/2 mice showed a notable increase in alternation percentage. The graph provides the data in the format of mean ± SEM (one-way ANOVA with post-hoc Dunnett test for R6/2 mice comparison; **$p < 0.01$). (**c**) Box and whisker plot

compared the average body weight for R6/2 mice over two time points with 7 days before viral injection surgery and 42 days after surgery. ND1+Dlx2 treated R6/2 mice lost less body weight when compared to the mCherry treated control R6/2 mice after 42 days post-surgery (*$p < 0.05$; unpaired Student's t-test).

Chapter 4

Discussion

Converting Striatal Astrocyte to GABAergic Neuron

In this paper, it was demonstrated that striatal astrocytes in R6/2 transgenic mice can be converted into GABAergic neurons in vivo to improve neurological and behavior phenotypes. The ND1 plus Dlx2 based gene therapy via intracranial injection in the striatum has been shown to notably alleviate motor deficits, improve short-term memory, and reduce the rate of weight loss. Utilizing the AAV5 GFAP::Cre system to limit viral expression to only astrocytes, nearly all of the ND1+Dlx2 infected cells were GFAP+ astrocytes in the early time points with little, if any, NeuN+ neurons. However, towards the later time points, ND1+Dlx2 infected cells were seen to no longer be GFAP+ astrocytes and instead found in NeuN+ neurons. Furthermore, neither the R6/2 AAV mCherry control nor the wild type group showed a transition from astrocyte to neuron in a time dependent manner with the lack of co-labeling in the NeuN and GFAP marker. All of this evidence suggests that direct in vivo conversion for the transition from astrocytes to neurons based on time is the most probable explanation for this phenomenon.

However, regardless of the evidence indicating in vivo cell conversion, there is still a concern with the possibility of the AAV5 vector being expressed through immunofluorescent markers in endogenous neurons instead of neurons converted from astrocytes. This issue would be a greater problem in the case if mCherry+ neurons colocalized with NeuN for the R6/2 mCherry control samples in the GFAP::cre system since they should not be able to convert astrocytes. These endogenous neurons could express the reporter protein through direct contact or even exosomes if the AAV5 system could express the Cre recombinase vector in these

endogenous neurons in order to invert the ND1 or Dlx2 coding sequence into its correct orientation. Thus, further research on the underlying mechanisms behind viral leakage into endogenous neurons is necessary to provide even stronger evidence for in vivo cell conversion in the central nervous system. A way to combat this concern would be to conduct more side-by-side control experiments with mCherry and ND1+Dlx2 at various time windows to better quantify any viral leakage. More interestingly, if a promotor was discovered to provide even higher specificity for astrocytes than the GFAP promoter currently used for the expression of cre, then the use of that different promoter for astrocyte to neuron conversion could more effectively resolve the concern with the possibility of viral leakage into endogenous neurons.

Despite the concern with the possibility of AAV5 vector expression in endogenous neurons, there was still greater concentration of neurons found in the striatum of R6/2 mice that received the ND1+Dlx2 treatment in comparison to the R6/2 mice that had the mCherry control treatment. This neurological phenotype was also expressed through behavioral differences between the R6/2 ND1 plus Dlx2 transduced mice and R6/2 mCherry-transduced control group. The ND1+Dlx2 treated R6/2 mice demonstrated significant increases in the distance traveled and alternation percentages when compared to the R6/2 mCherry-transduced control group which indicate that there were physically observable improvements in motor function and spatial learning. Furthermore, the lower rate of weight loss observed in the ND1+Dlx2 treated R6/2 mice compared to the R6/2 mCherry-transduced control group highlighted the possibility that the ND1+Dlx2 gene therapy treatment could slow the progression of Huntington's disease.

In addition to the approach used with stereotaxic intracranial injection in the striatum, another virus labeling system in the form of the retro-orbital route has also shown some promise in reaching global astrocytes-specific targeting for conversion. The Cre-FLEx system via retro-

orbital injection was demonstrated to have a wide reach in virus infection across multiple brain regions and the spinal cord. For the ND1+Dlx2 treatment through retro-orbital injection, there was evidence of neuron regeneration with the greater density of NeuN and more intense Cux1 signal compared to the control group, indicating that some restoration of neurons occurred in the superficial layer of the cerebral cortex. Furthermore, the R6/2 ND1 plus Dlx2 transduced mice also showed the presence of GFP and ChAT double positive cells co-labeled with NeuN which provided evidence indicating that the ND1+Dlx2 treatment through retro-orbital injection led to the presence of converted cholinergic neurons in the striatum.

Conclusion, Considerations, and Implications

Even with the increase in neuron concentration along with improvements in behavioral and neurological phenotypes, there is still much more research that needs to be conducted in order to provide further evidence for the beneficial effects of the potentially disease-modifying therapy. For the in vivo converted neurons, more research needs to be done on whether these converted neurons demonstrate the same electrophysiological properties to the preexisting neurons. If so, there is also a question of whether the proper neurons are generated in the correct region that can then project to the right targets in forming proper circuits during the process of repair in the central nervous system. Furthermore, in converting from astrocytes to neurons, more work needs to be done to better understand the effects this process has on the concentration of astrocytes surrounding neurons in the local environment. In addition to regenerating GABAergic neurons, the possibility of generating a greater variety of neuronal subtypes with varying transcription factor combination should also be further researched. In addition to examining the

underlying disease markers, a larger sample size and greater variety in behavioral tests should be conducted to better quantify the specific phenotypic improvements observed from the R6/2 ND1 plus Dlx2 transduced mice.

Another source of limitation for the in vivo cell conversion technology involves the underlying gene mutation pervasive in Huntington's disease since even the converted GABAergic neurons may still eventually exhibit aggregation of mutant HTT that can then lead to neurodegeneration since astrocyte conversion to neurons does not directly resolve the systemic issue regarding the length of the CAG trinucleotide repeat sequence. Thus, further work into a more holistic solution can involve the combination in the use of the in vivo cell conversion technology to alleviate the symptoms or slow the disease progression and CRISPR gene editing to fix the huntingtin gene expansion. That way, both the gene mutation and the neurodegeneration issue can be properly addressed in providing an effective therapeutic treatment solution to Huntington's disease.

Without a doubt, the data provided in this paper demonstrate not only the conversion of striatal astrocytes into GABAergic neurons at a cellular level but also the neurological and behavioral improvements in motor skills, spatial learning, and weight loss. However, more data sets and experimental trials must be conducted to more conclusively prove and further these conclusions. The ND1 plus Dlx2 gene therapy technology preliminarily demonstrates great potential in treating Huntington's disease and various other neurodegenerative disorders. Since the current available treatments for Huntington's disease merely reduces the severity for only certain symptoms, the in vivo cell conversion technology provides the possibility for regenerating neurons to more effectively address or slow the progression of the neurodegenerative disease.

BIBLIOGRAPHY

(1) Venuto, C. S., & Kieburtz, K. Huntington disease. *Oxford Medicine Online*. (2017). doi:10.1093/med/9780199937837.003.0008

(2) HD Collaborative Research Group. A novel gene containing a trinucleotide repeat that is expanded and unstable on Huntington's disease chromosomes. *Cell* 72: 971-983 (1993).

(3) de Die-Smulders CE, de Wert GM, Liebaers I, Tibben A, Evers-Kiebooms G. Reproductive options for prospective parents in families with Huntington's disease: clinical, psychological and ethical reflections. *Human Reproduction Update*. 19 (3): 304–15. (2013). doi:10.1093/humupd/dms058

(4) Mangiarini, L. et al. Exon 1 of the HD gene with an expanded CAG repeat is sufficient to cause a progressive neurological phenotype in transgenic mice. *Cell* 87, 493–506 (1996)

(5) Bates GP, Dorsey R, Gusella JF, Hayden MR, Kay C, Leavitt BR, Nance M, Ross CA, Scahill RI, Wetzel R, Wild EJ, Tabrizi SJ "Huntington disease". *Nature Reviews Disease Primers*. 1: 15005. (2015). doi:10.1038/nrdp.2015.5

(6) Rikani, A. A. et al. The mechanism of degeneration of striatal neuronal subtypes in Huntington disease. Ann. *Neurosci*. 21, 112–114 (2014).

(7) Frank S. "Treatment of Huntington's disease". *Neurotherapeutics*. 11 (1): 153–60. (2014). doi:10.1007/s13311-013-0244-z

(8) Ross, C. A. et al. Huntington disease: natural history, biomarkers and prospects for therapeutics. *Nat. Rev. Neurol*. 10, 204-216 (2014).

(9) Beighton P, Hayden MR. Huntington's chorea. *S Afr Med J* 59: 250 (1981).

(10) Frank S, Jankovic J. "Advances in the pharmacological management of Huntington's disease". *Drugs*. 70 (5): 561–71. (2010). doi:10.2165/11534430-000000000-00000

(11) Dickey AS, La Spada AR. "Therapy development in Huntington disease: From current strategies to emerging opportunities". *American Journal of Medical Genetics*. Part A. 176 (4): 842–861. (2018). doi:10.1002/ajmg.a.38494

(12) Bates GPHP, Jones AL. *Huntington's Disease*. Oxford, UK: Oxford Univ. Press, 2002

(13) Politis M, Pavese N, Tai YF, Tabrizi SJ, Barker RA, Piccini P. Hypothalamic involvement in Huntington's disease: an in vivo PET study. *Brain* 131: 2860-2869, 2008

(14) Rosenblatt A. Neuropsychiatry of Huntington's disease. *Dialogues Clin Neurosci* 9: 191-197, 2007

(15) Walker FO. "Huntington's disease". *Lancet*. 369 (9557): 218–28. (2007). doi:10.1016/S0140-6736(07)60111-1

(16) Harper PS. "Huntington's disease: a clinical, genetic and molecular model for polyglutamine repeat disorders". *Philosophical Transactions of the Royal Society of London. Series B, Biological Sciences.* 354 (1386): 957–61. (1999). doi:10.1098/rstb.1999.0446

(17) Beighton P, Hayden MR. Huntington's chorea. *S Afr Med J* 59: 250, 1981

(18) Conneally PM. Huntington disease: genetics and epidemiology. *Am J Hum Genet* 36: 506-526, 1984

(19) Morrison, P. J., Harding-Lester, S. & Bradley, A. Uptake of Huntington disease predictive testing in a complete population. *Clin. Genet*. 80, 281-286

(20) Fisher, E. R. & Hayden, M. R. Multisource ascertainment of Huntington disease in Canada: prevalence and population at risk. *Mov. Disord.* 29, 105-114 (2014)

(21) Reiner A, Albin RL, Anderson KD, D'Amato CJ, Penney JB, Young AB. Differential loss of striatal projection neurons in Huntington disease. *Proc Natl Acad Sci USA* 85: 5733-5737, 1988

(22) Caron, N. S., Wright, G., & Hayden, M. R. (1998). Huntington Disease. In M. P. Adam (Eds.) et. al., *GeneReviews*. University of Washington, Seattle.

(23) Zuccato, C., Valenza, M., & Cattaneo, E. Molecular Mechanisms and Potential Therapeutical Targets in Huntington's Disease. *Physiological Reviews, 90*, 905-981. (2010). doi:10.1152/physrev.00041.2009.

(24) Dayalu P, Albin RL. "Huntington disease: pathogenesis and treatment". *Neurologic Clinics.* (2015). 33 (1): 101–14. doi:10.1016/j.ncl.2014.09.003

(25) Xu, M., & Wu, Z. Y. Huntington Disease in Asia. Chinese medical journal, 128(13), 1815–1819. (2015). https://doi.org/10.4103/0366-6999.159359

(26) Harper P, In Bates G, Harper P, Jones L. "The epidemiology of Huntington's disease". Huntington's Disease – Third Edition. *Oxford: Oxford University Press*. pp. 159–189. (2002).

(27) Bates, G., Dorsey, R., Gusella, J. et al. Huntington disease. *Nature Review Disease Primers* 1, 15005 (2015). https://doi.org/10.1038/nrdp.2015.5

(28) Quin L, Busee M. "Development of physiotherapy guidance and treatment-based classifications for people with Huntington's disease". *Neurodegenerative Disease Management*. 2 (1): 21–31. (2012). doi:10.2217/nmt.11.86

(29) Aziz NA, Jurgens CK, Landwehrmeyer GB, can Roon-Mom WM, van Ommen GJ, Stijnen T, Roos RA, Orth M, Handley OJ, Schewenke C, Ho A, Wild EJ, Tabrizi SJ,

Landwehrmeyer GB. Normal and mutant HTT interact to affect clinical severity and progression in Huntington disease. *Neurology* 73: 1280-1285, 2009

(30) Claassen, D. O. et al. Tetrabenazine treatment patterns and outcomes for chorea associated with Huntington disease: a retrospective chart review. *J. Huntingt. Dis*. 7, 345–353 (2018).

(31) Tang TS, Chen X, Liu J, Bezprozvanny I. Dopaminergic signaling and striatal neurodegeneration in Huntington's disease. *J Neurosci* 27: 7899-7910, 2007

(32) Frank S, Ondo W, Fahn S, Hunter C, Oakes D, Plumb S, Marshall F, Shoulson I, Eberly S, Walker F, Factor S, Hunt V, Shinaman A, Jankovic J. A study of chorea after tetrabenazine withdrawal in patients with Huntington disease. *Clin Neuropharmacol* 31: 127-133 , 2008.

(33) Citrome L. "Breakthrough drugs for the interface between psychiatry and neurology". *International Journal of Clinical Practice*. 70 (4): 298–9. (2016). doi:10.1111/ijcp.12805

(34) Buehr M, Meek S, Blair K, Yang J, Ure J, Silva J, McLay R, Hall J, Ying QL, Smith A. Capture of authentic embryonic stem cells from rat blastocysts. *Cell* 135: 1287-1298, 2008.

(35) Aubry L, Bugi A, Lefort N, Rousseau F, Peschanski M, Perrrier AL. Striatal progenitors derived from human ES cells mature into DARPP32 neurons in vitro and in quinolinic acid-lesioned rats. Proc Natl Acad Sci USA 105: 16707-16712, 2008

(36) Dunnett SB, Rosser AE. Cell transplantation for Huntington's disease. Should we continue? *Brain Res Bull* 72: 132-147, 2007.

(37) Guo, Z. Y. et al. In vivo direct reprogramming of reactive glial cells into functional neurons after brain injury and in an Alzheimer's disease model. *Cell Stem Cell* 14: 188–202, 2014.

(38) Niu, W. et al. In vivo reprogramming of astrocytes to neuroblasts in the adult brain. *Nat. Cell Biol*. 15, 1164–1175, 2013.

(39) Bachoud-Levi AC, Remy P, Nguyen JP, Brugieres P, Lefaucheur JP, Bourdet C, Baudic S, Gaura V, Maison P, Haddad B, Boisse MF, Grandmougin T, Jeny R, Bartolomeo P, Dalla Barba G, Degos JD, Lisovoski F, Ergis AM, Pailhous E, Cesaro P, Hantraye P, Peschanski M. Motor and cognitive improvements in patients with Huntington's disease after neural transplantation. Lancet 356: 1975-1979, 2000.

(40) Taylor, C. J., Bolton, E. M., & Bradley, J. A. Immunological considerations for embryonic and induced pluripotent stem cell banking. *Philosophical transactions of the Royal Society of London. Series B, Biological sciences*, 366(1575), 2312–2322. (2011). https://doi.org/10.1098/rstb.2011.0030

(41) Büning, H., & Schmidt, M. Adeno-associated Vector Toxicity-To Be or Not to Be?. *Molecular therapy : the journal of the American Society of Gene Therapy*, 23(11), 1673–1675. (2015). https://doi.org/10.1038/mt.2015.182

(42) Liu, Y. G. et al. Ascl1 converts dorsal midbrain astrocytes into functional neurons in vivo. *J. Neurosci*. 35: 9336–9355, 2015.

(43) Chan KY, Jang MJ, Yoo BB, Greenbaum A, Ravi N, Wu WL, Sánchez-Guardado L, Lois C, Mazmanian SK, Deverman BE, and Gradinaru V. Engineered AAVs for efficient noninvasive gene delivery to the central and peripheral nervous systems. *Nat Neurosci*. 20(8): 1172–1179. (2017). doi:10.1038/nn.4593.

(44) Guo, Z., Zhang, L., Wu, Z., Chen, Y., Wang, F., & Chen, G. In vivo direct reprogramming of reactive glial cells into functional neurons after brain injury and in an Alzheimer's disease model. *Cell Stem Cell*, 14(2), 188-202. (2014). doi:10.1016/j.stem.2013.12.001

(45) Sun, A., Yuan, Q., Tan, S., Xiao, Y., Wang, D., Khoo, A., . . . Je, H. Direct induction and functional maturation of forebrain GABAergic neurons from human pluripotent stem cells. *Cell Reports*, 16(7), 1942-1953. (2016). doi:10.1016/j.celrep.2016.07.035

(46) Li, H., & Chen, G. In vivo reprogramming for CNS repair: Regenerating neurons from endogenous glial cells. *Neuron*, 91(4), 728-738. (2016). doi:10.1016/j.neuron.2016.08.004

(47) Tang, X., Zhou, L., Wagner, A. M., Marchetto, M. C., Muotri, A. R., Gage, F. H., & Chen, G. Astroglial cells regulate the developmental timeline of human neurons differentiated from induced pluripotent stem cells. Stem Cell Research, 11(2), 743-757. (2013). doi:10.1016/j.scr.2013.05.002

(48) Van der Burg, J. M., Björkqvist, M., & Brundin, P. Beyond the Brain: WIDESPREAD pathology in Huntington's disease. *The Lancet Neurology, 8*(8), 765-774. (2009). doi:10.1016/s1474-4422(09)70178-4

(49) Chen, G., Wernig, M., Berninger, B., Nakafuku, M., Parmar, M., & Zhang, C. In vivo reprogramming for brain and spinal cord repair. *Eneuro*, 2(5). (2015). doi:10.1523/eneuro.0106-15.2015

(50) Chen, Y., Ma, N., Pei, Z., Wu, Z., Do-Monte, F. H., Keefe, S., . . . Chen, G. A NeuroD1 AAV-based gene therapy for functional Brain repair AFTER Ischemic injury through in Vivo Astrocyte-to-Neuron Conversion. *Molecular Therapy*, 28(1), 217-234. (2020). doi:10.1016/j.ymthe.2019.09.003

(51) Wu, Z., Parry, M., Hou, X., Liu, M., Wang, H., Cain, R., . . . Chen, G. Gene therapy conversion of striatal astrocytes into GABAergic neurons in mouse models of Huntington's disease. *Nature Communications*, 11(1). (2020). doi:10.1038/s41467-020-14855-3F

(52) Poulin G, Turgeon B, Drouin J. "NeuroD1/beta2 contributes to cell-specific transcription of the proopiomelanocortin gene". *Molecular and Cellular Biology*. 17 (11): 6673–82. (1997). doi:10.1128/mcb.17.11.6673

(53) Ozcelik T, Porteus MH, Rubenstein JL, Francke U. "DLX2 (TES1), a homeobox gene of the Distal-less family, assigned to conserved regions on human and mouse chromosomes 2". *Genomics*. 13 (4): 1157–61. (1992). doi:10.1016/0888-7543(92)90031-M

(54) Roedel A, Storch C, Holsboer F, Ohl F. Effects of light or dark phase testing on behavioural and cognitive performance in DBA mice. *Lab Anim*. (2006) Oct;40(4):371-81. doi: 10.1258/002367706778476343. PMID: 17018208.

(55) Kraeuter AK., Guest P.C., Sarnyai Z. (2019) The Y-Maze for Assessment of Spatial Working and Reference Memory in Mice. In: Guest P. (eds) Pre-Clinical Models. *Methods in Molecular Biology*, vol 1916. Humana Press, New York, NY. https://doi.org/10.1007/978-1-4939-8994-2_10

ACADEMIC VITA

EDUCATION

The Pennsylvania State University **State College, PA**
Smeal College of Business | Bachelor of Science in Finance *Class of 2021*
Schreyer Honors College
Awards: Evan Pugh Scholar Senior Award, Sharbaugh Honors Scholarship, The President's Freshman Award, The President Sparks Award, Dean's List (Fall 2017 – Present)

RELEVANT EXPERIENCE

Chen Lab, Charles H. "Skip" Smith Life Sciences Laboratory **State College, PA**
Undergraduate Research Assistant *Aug 2018 – Sept 2020*

- Worked under Zhuofan on the Traumatic Brain Injury project to set up a mouse model to mimic the traumatic brain injuries that occur in sports players, to achieve the reconstruction of neural networks in motor cortex after closed head injury, and to unveil the mechanisms underlying the treatment process in the CHI model
- Worked under Xiaoyi on the Huntington's Disease project with R6/2 HD mouse models to determine the efficacy of in-vivo cell conversion technology using AAV-mediated ectopic expression of Dlx2 and ND1 transcription factors to convert striatal astrocytes into GABAergic neurons
- Performed neurological impact tests, intracranial viral injection surgery, perfusion, behavioral studies for mice, brain sectioning, fluorescent immunostaining, and confocal imaging of the stained brain slices
- Worked on in-vivo brain repair by converting reactive glial cells to functional neuron cells from ND1 expression

Department of Biology **State College, PA**
Teaching Assistant *Jan 2019 – Present*

- Ran an entire laboratory section of Biol 230W and Biol 110 that consisted of 24 undergraduate students by giving lectures on all pre-lab logistics and biological concepts, guiding experimental procedures, grading all assignments, and holding office hours
- Supervised all laboratory activities for Biol 230W and Biol 110 in collaboration with faculty by maintaining a safe, instructive environment in the laboratory at all times by following and enforcing all safety guidelines in the laboratory

Department of Chemistry **State College, PA**
Learning Assistant *Jan 2019 – Present*

- Attended weekly Chem 210 and Chem 202 lectures to provide guidance for students with organic chemistry concepts presented in class especially through clicker questions and group problems
- Led weekly workshops independently to foster a collaborative learning environment directly for students to emphasize key topics discussed in lecture

LEADERSHIP & ACTIVITIES

Penn State Alternative Breaks **State College, PA**
Site Leader *Jan 2018 – Dec 2018*

- Participated in the Alternative Spring Break trip to Cleveland to teach refugees, package meals at a food bank, build sheds at Habitats for Humanity, volunteer at nursing homes, and clean rundown buildings

- Led the Fall Alternative Break trip to Camden, New Jersey as a Site Leader to teach participants the social justice topic of environmental injustices by volunteering at food banks and gardens

Mid-State Literacy Council **State College, PA**
ESL Tutor *Jan 2018 – Dec 2019*

- Provided one-on-one tutoring for adult English as a Second Language students or Adult Basic Education learners who want to improve reading, writing, or computer literacy skills or work towards a GED
- Helped adults improve conversation and comprehension skills, expand vocabularies, and understand American culture while emphasizing health literacy in English for adults to successfully interact with health care professionals they will encounter

Christian Medical and Dental Associations Undergraduate Penn State Chapter **State College, PA**
Founder and Treasurer *Sept 2020 – Present*

- Established the Penn State Undergraduate Chapter of CMDA to extend the services of the parent organization to undergraduate students across multiple STEM fields
- Organized guest speaker sessions for Christian professionals in the medical and dental field to provide insight into the integration of their career paths and faith
- Led bimonthly general body meetings to cultivate a Christian Community across multiple campus ministries for undergraduate students who shared similar vocational interests

RELEVANT COURSEWORK & SKILLS

Relevant Coursework: Anatomy and Physiology, Organic Chemistry, Genetics, Biochemistry, Molecular Biology
Skills: Fluent in Mandarin, Proficient in Microsoft Excel, Experienced in Suturing, Proficient with Gephi and Tableau software for data visualization and analysis